OPEN ACCESS
World Journal of Multidisciplinary Studies
ISSN: 3049-0855 | Vol. 2, No. 5, 2025
Website: https://wasrpublication.com/wjms/

EFFECTS OF VARIATION IN WATER SOLUBLE AEROSOL CONCENTRATIONS AND RELATIVE HUMIDITY IMPACT ON THE POLARIZABILITY AND PHASE FUNCTION OF URBAN ATMOSPHERE

A. Aliyu[1*], B. I. Tijjani[2] and U. M. Gana[2]

[1] Department of Physics, Aliko Dangote University of Science and Technology Wudil, Kano State, Nigeria.

[2] Department of Physics, Bayero University Kano, Kano State, Nigeria.

Received: 11/04/2025 | Accepted: 01/05/2025 | Published: 20/05/2025

Abstract: This research investigates how changes in water-soluble aerosol concentrations and relative humidity (RH) affect the optical properties of irregularly-shaped urban aerosols. Using the Optical Properties of Aerosols and Clouds software (OPAC 4.0), urban aerosol optical properties at visible wavelengths (0.4-0.8 μm) were simulated across eight relative humidities (0%,50%,70%,80%,90%,95%,98%,99%). We applied Stokes parameters to calculate phase functions and combined Claussi-Massoti formulation with Maxwell and Lorentz-Lorentz relations were used for computation of effective polarizabilities. The results reveal new information on how RH and aerosol concentration impact urban aerosol optical properties. Notably, we determined effective polarizabilities, polarization, and phase function data using OPAC 4.0 and determined aerosol size growth curves' mean exponent through effective hygroscopic growth. Effective polarizability exhibits a decrease with increasing wavelength and water-soluble aerosols concentration, whereas it increases with rising relative humidity. Phase function decreases with the increase in wavelength and also, decreases with the increase in scattering angle, satisfies power law. When all the plots were compared, phase functions increase with the increase in relative humidity, increases with the increase in the concentration of water-soluble aerosols.

Keywords: aerosols, polarization, polarizability, and phase function.

Cite this article:

Aliyu, A., Tijjani, B. I., and Gana, U. M., (2025). EFFECTS OF VARIATION IN WATER SOLUBLE AEROSOL CONCENTRATIONS AND RELATIVE HUMIDITY IMPACT ON THE POLARIZABILITY AND PHASE FUNCTION OF URBAN ATMOSPHERE. *World Journal of Multidisciplinary Studies, 2*(5), 19-34.

1 Introduction

Urban areas are significant sources of air pollution, emitting a diverse array of aerosols into the atmosphere. These aerosols exhibit complex shapes, ranging from simple geometric structures to intricate non-spherical configurations. Understanding the optical properties of these aerosols, including their polarizability and phase function, is crucial for accurately assessing their impacts on climate, visibility, and human health. The polarizability of an aerosol particle refers to its ability to polarize incident light, influenced by factors such as size, shape, refractive index, and composition (Mishchenko *et al*., 2002). The phase function, describes the angular distribution of scattered light by an aerosol particle, providing essential information for radiative transfer calculations and remote sensing applications. Despite ongoing research efforts, estimating the effects of aerosols on the atmospheric energy budget remains a significant uncertainty (Anderson *et al*., 2003). Accurate methods for aerosol identification and characterization are lacking, hindering our understanding of aerosol physics (Anderson *et al.*, 2003; Schwartz and Andreae, 1996). To address this knowledge gap, various methods and models have been developed to determine the polarizability and phase function of urban non-spherical aerosols. The OPAC 4.0 (Optical Properties of Aerosols and Clouds) model, version 4.0 (Koepke *et al*., 2015), is a widely used tool that employs Mie theory to simulate the optical properties of aerosols (Hess, Koepke, and Schult, 1998). Several studies have investigated the optical properties of aerosols, including their polarizability and phase function (Smith and Johnson, 2010; Mishchenko *et al*., 2002). However, a specific examination of the polarizability and phase function of urban non-spherical aerosols using OPAC remains a crucial research gap.

This study aims to fill this gap by applying OPAC to simulate the polarizability and phase function of urban non-spherical aerosols. The comprehensive simulations will provide valuable insights into the scattering patterns and polarization behaviour of these aerosols at different scattering angles. This information is essential for understanding the impact of aerosols on atmospheric radiation balance, air quality, and climate in urban areas.

2 Methodology

The approach to be employed for analysing the OPAC 4.0 dataset to fulfil the research objectives is outlined.

2.1 OPAC 4.0

The OPAC software, developed by Hess *et al*. (1998), is a crucial tool for climate modelling, offering extensive datasets on atmospheric aerosol optical properties. Its user-friendly interface

***Corresponding Author**
Aliyu Aliyu*
Department of Physics, Aliko Dangote University of Science and Technology Wudil, Kano State, Nigeria.

and FORTRAN program enable efficient computation of optical properties for various cloud and aerosol combinations, simplifying the modelling process. This study employs OPAC to generate urban aerosol model variants across eight relative humidity levels (0%, 50%, 70%, 80%, 90%, 95%, 98%, 99%) and wavelengths spanning 0.25-40 micrometres. Urban aerosols are composed of three components: water-soluble, insoluble, and soot. The software combines these components to create aerosol types. The study systematically varies the concentration of water-soluble components while keeping insoluble and soot components constant. Five models were developed, each with increasing water-soluble component concentrations (30% relative to the base model). The OPAC FORTRAN program calculates the optical properties for each model. The extracted optical properties from OPAC 4.0 include extinction coefficient, scattering coefficient, absorption coefficient, single scattering albedo, and asymmetric parameters. These properties are obtained at all relative humidity levels and spectral wavelengths (0.4-0.8 µm).

The models extracted from OPAC 4.0 are given in table 1

Table 1 the microphysical properties of the urban aerosols at 0% RH (Hess *et al*, 1998).

Components	R_{min} (µm)	R_{max} (µm)	Sigma	R_{dry} (µm)
Waso	0.005	20.00	2.24	0.0212
Inso	0.005	20.00	2.51	0.4710
Soot	0.005	20.00	2.00	0.0118

Table 2: Five Model Component Mixtures with Varying Water-Soluble (WASO) Aerosol Concentrations.

	Model 1	Model 2	Model 3	Model 4	Model 5
Components	No.Den (cm^{-3})	No. Den(cm^{-3})	No.Den(cm^{-3})	No. Den(cm^{-3})	No. Den(cm^{-3})
INSO	1.50	1.50	1.50	1.50	1.50
WASO	**28,000.00**	**36,400.00**	**44,800.00**	**53,200.00**	**61,600.00**
SOOT	130,000.00	130,000.00	130,000.00	130,000.00	130,000.00

Table 2 describes the urban aerosols simulated with varying water soluble (non-spherical) component. The number concentrations were increased by adding 30% of model 1 model to subsequent models.

2.2 Polarizability

From Shettle and Fenn, (1979), the well-known Lorentz - Lorentz relation between the refractive index n and polarizability α is given as

$$\alpha = \frac{3(n^2-1)}{\rho(n^2+2)} \quad (1)$$

when the material has absorbing properties the refractive index is expressed as complex number $n = n' + ik$, where n is the complex refractive index of the material, n' is the real part of the refractive index, representing the material's ability to bend light (also known as the refractive index in non-absorbing materials), i is the imaginary unit, which satisfies $i^2 = -1$, k the imaginary part of the refractive index, representing the material's ability to absorb light (also known as the extinction coefficient), and ρ is the number density.

Equation (1) gives the polarizability of one type of aerosol, to determine the effective polarizability of the mixture the following addition relation is used.

$$\alpha_{eff} = \sum_{i=1}^{n} V_i \alpha_i \quad (2)$$

where α_{eff} is the effective polarizability of the mixtures, V_i is the volume mix ratio of the i^{th} aerosol component, α_i is the polarizability of i^{th} component.

2.3 Phase functions

The function $F_{11}(\Theta)$ is called the phase function and is normalized to 1 such that (Lindqvist *et al.*, 2014),

$$\frac{1}{2}\int_0^{\pi} \sin(\Theta) F_{11}(\Theta) d\Theta = 1 \quad (3)$$

where Θ is the scattering angle, $F_{11}(\Theta)$ is proportional to the scattered intensity as a function of the scattering angle. It describes the angular distribution of the scattered light by aerosols, and provides information about the relative intensity and directionality of scattered light at different scattering angles.

3. Results and Discussions

The graphs of phase functions with scattering angles and effective polarizabilities with wavelengths (0.4 to 0.8 µm) at eight relative humidities are presented. The graphs are presented as figures (a) and figures (b). The figures (a) displays the phase function plots from 0 to 180 degrees. However, due to the dense packing of the plots, Figure (b) is used to illustrate the effect of forward scattering angles on the phase functions.

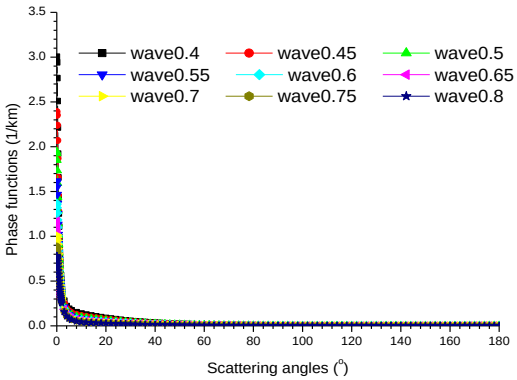

Figure 1(a): A graph of Phase functions against scattering angles at 0% RH WASO Model 1

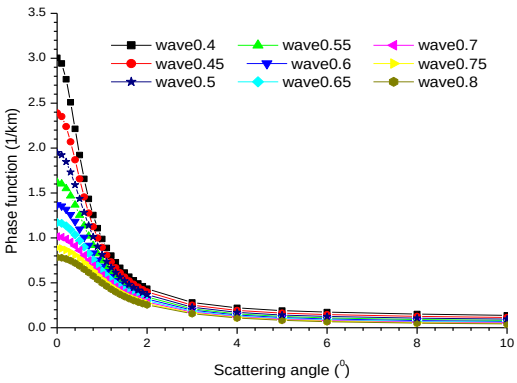

Figure 1(b): A graph of Phase functions against scattering angles at 0% RH WASO Model 1

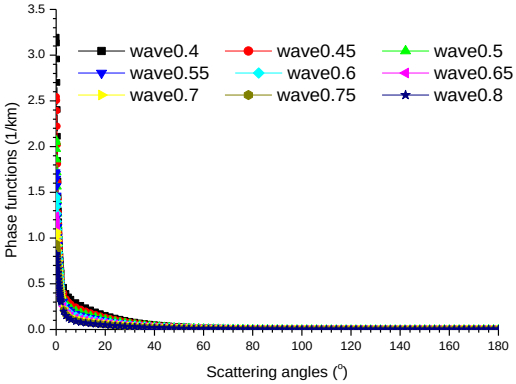

Figure 2(a): A graph of Phase functions against scattering angles at 50% RH WASO Model 1

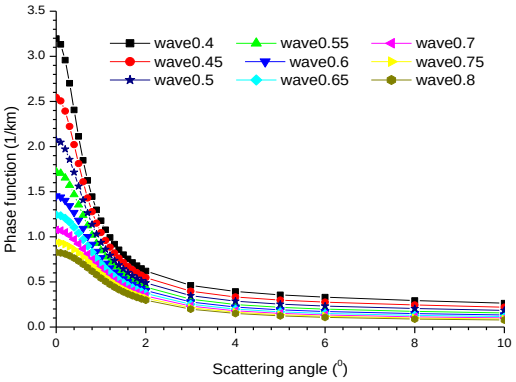

Figure 2(b): A graph of Phase functions against scattering angles at 50% RH WASO Model 1

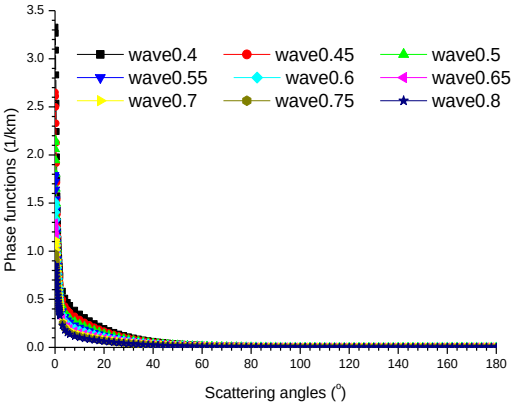

Figure 3(a): A graph of Phase functions against scattering angles at 70% RH WASO Model 1

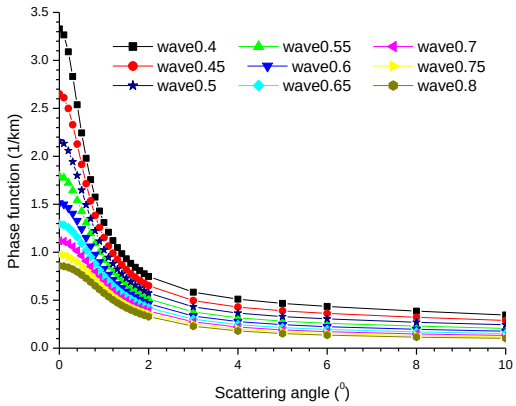

Figure 3(b): A graph of Phase functions against scattering angles at 70% RH WASO Model 1

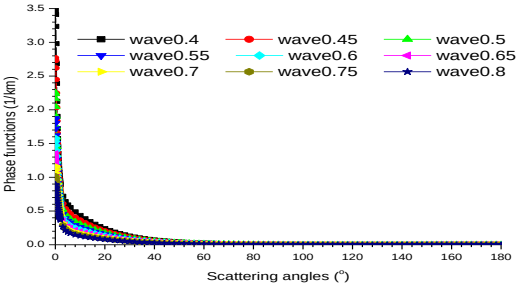

Figure 4(a): A graph of Phase functions against scattering angles at 80% RH WASO Model 1

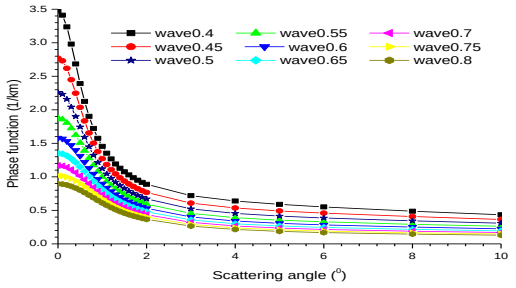

Figure 4(b): A graph of Phase functions against scattering angles at 80% RH WASO Model 1

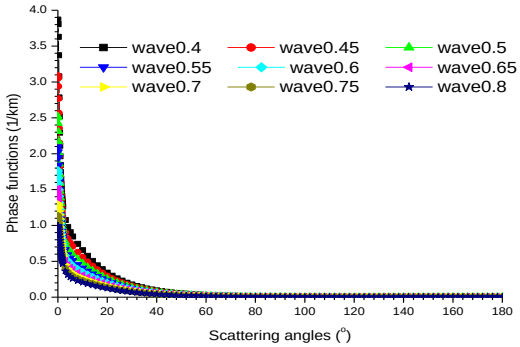

Figure 5(a): A graph of Phase functions against scattering angles at 90% RH WASO Model 1

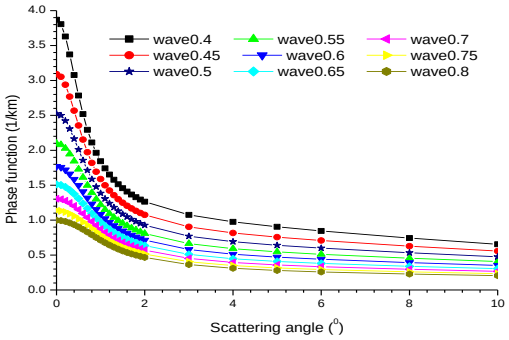

Figure 5(b): A graph of Phase functions against scattering angles at 90% RH WASO Model 1

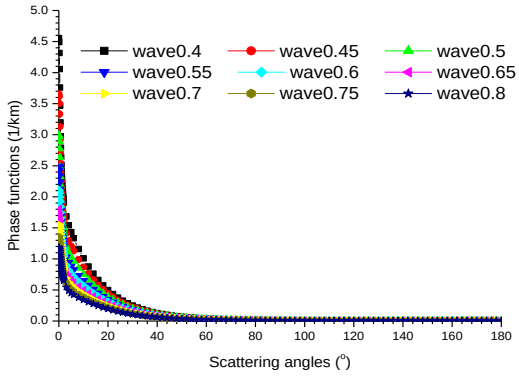

Figure 6(a): A graph of Phase functions against scattering angles at 95% RH WASO Model 1

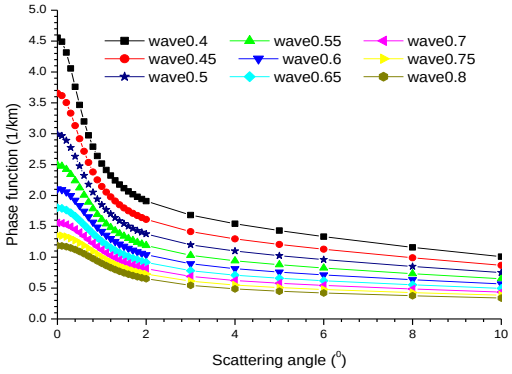

Figure 6(b): A graph of Phase functions against scattering angles at 95% RH WASO Model 1

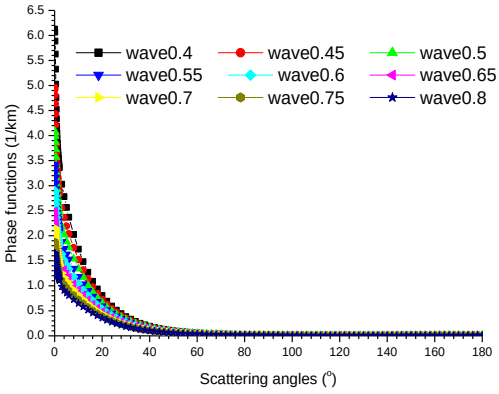

Figure 7(a): A graph of Phase functions against scattering angles at 98% RH WASO Model 1

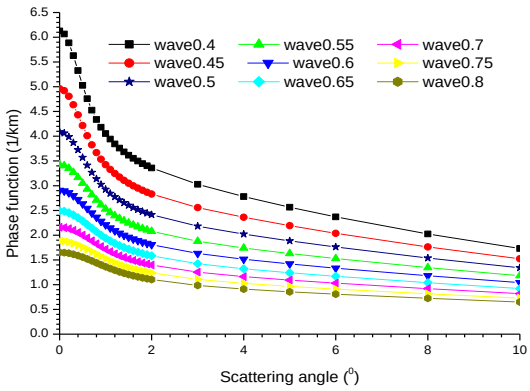

Figure 7(b): A graph of Phase functions against scattering angles at 98% RH WASO Model 1

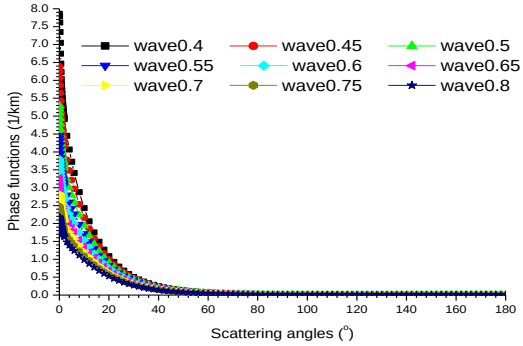

Figure 8(a): A graph of Phase functions against scattering angles at 99% RH WASO Model 1

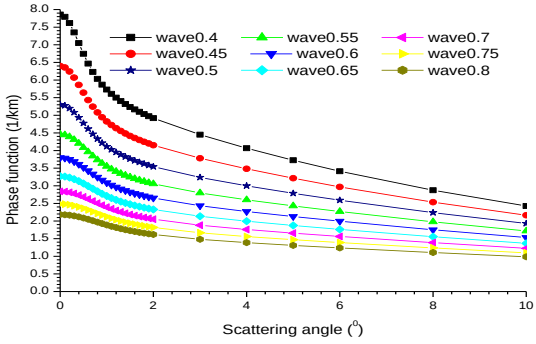

Figure 8(b): A graph of Phase functions against scattering angles at 99% RH WASO Model 1

Figures 1-8 demonstrate that the phase functions decrease with increasing scattering angles, adhering to the inverse power law. The phase functions are more pronounced at lower scattering angles because as the scattering angles increase, the scattering cross-section for forward scattering decreases, resulting in a reduced phase function. When all the plots are compared, it is evident that the phase function increases with increasing relative humidity RH. This is attributed to aerosol swelling due to water uptake, which increases the scattering cross-section and enhances forward scattering. The phase function decreases with increasing wavelength because longer wavelengths are more susceptible to aerosol absorption. This increased absorption reduces the amount of scattered light, leading to a decrease in forward scattering as the wavelength increase and consequently, a reduction in the phase function, as can be seen from figures 1b-8b.

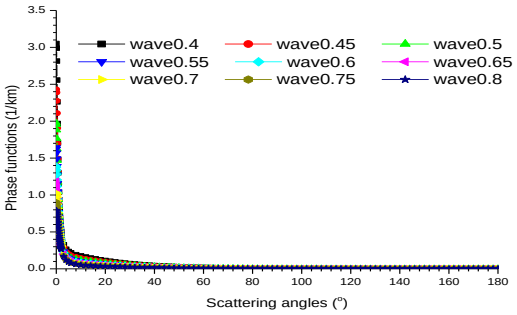

o

Figure 9(a): A graph of Phase functions against scattering angles at 0% RH WASO Model 2

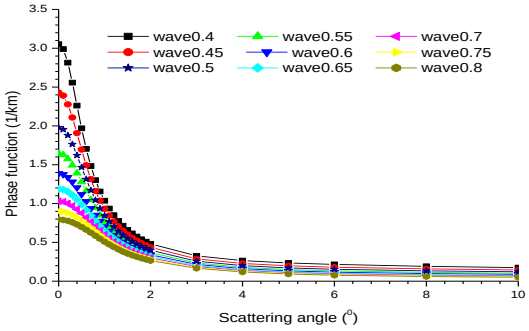

Figure 9(b): A graph of Phase functions against scattering angles at 0% RH WASO Model 2

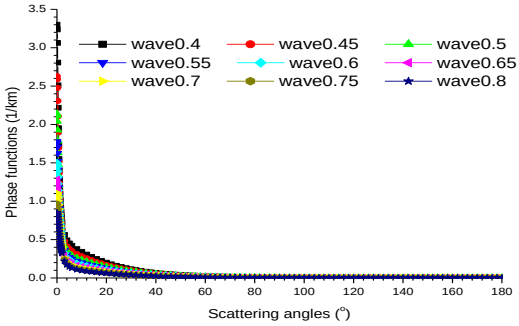

Figure 10(a): A graph of Phase functions against scattering angles at 50% RH WASO Model 2

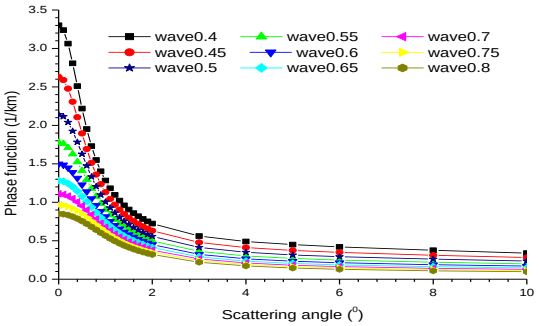

Figure 10(b): A graph of Phase functions against scattering angles at 50% RH WASO Model 2

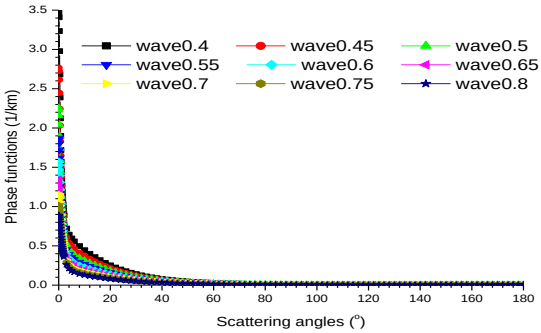

Figure 11(a): A graph of Phase functions against scattering angles at 70% RH WASO Model 2

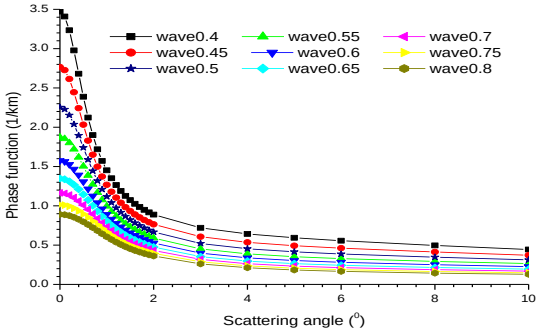

Figure 11(b): A graph of Phase functions against scattering angles at 70% RH WASO Model 2

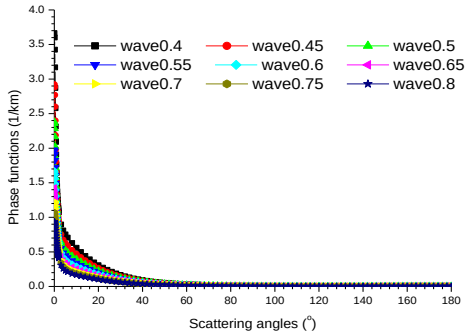

Figure 12(a): A graph of Phase functions against scattering angles at 80% RH WASO Model 2

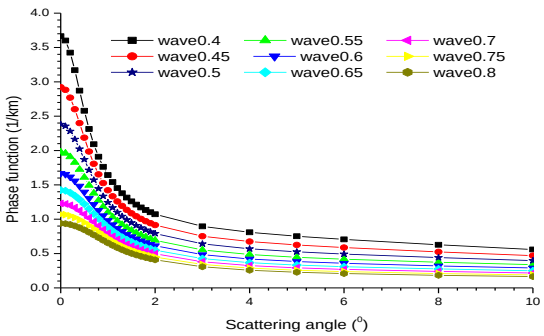

Figure 12(b): A graph of Phase functions against scattering angles at 80% RH WASO Model 2

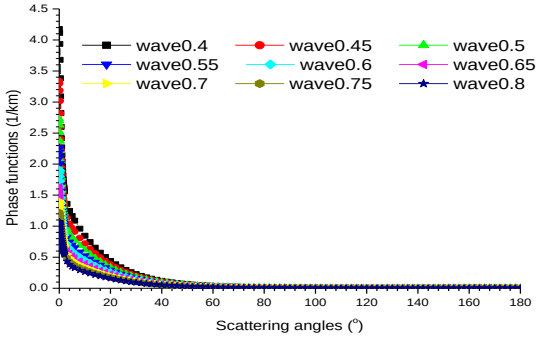

Figure 13(a): A graph of Phase functions against scattering angles at 90% RH WASO Model 2

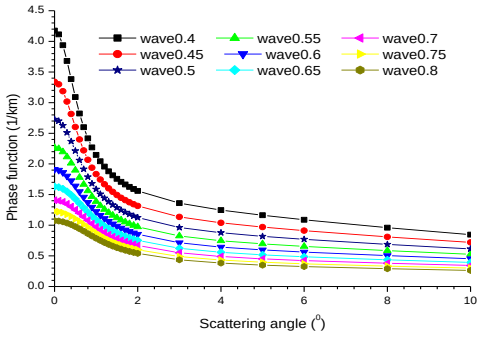

Figure 13(b): A graph of Phase functions against scattering angles at 90% RH WASO Model 2

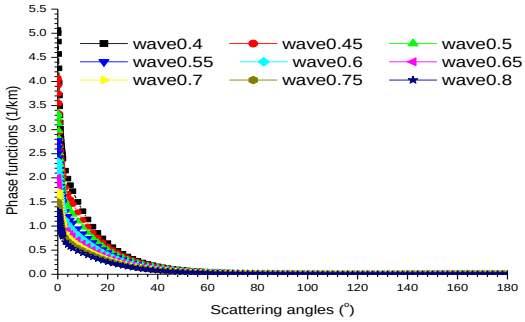

Figure 14(a): A graph of Phase functions against scattering angles at 95% RH WASO Model 2

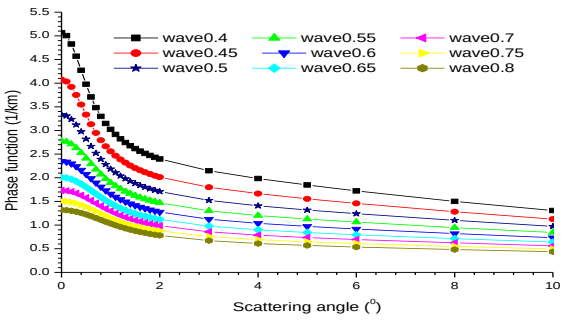

Figure 14(b): A graph of Phase functions against scattering angles at 95% RH WASO Model 2

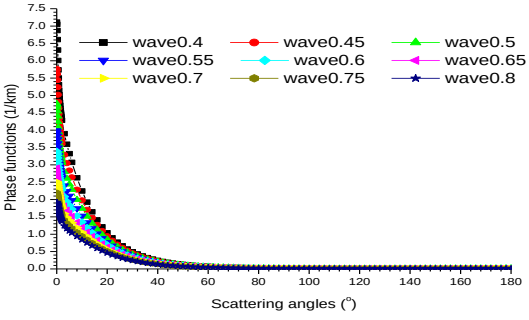

Figure 15(a): A graph of Phase functions against scattering angles at 98% RH WASO Model 2

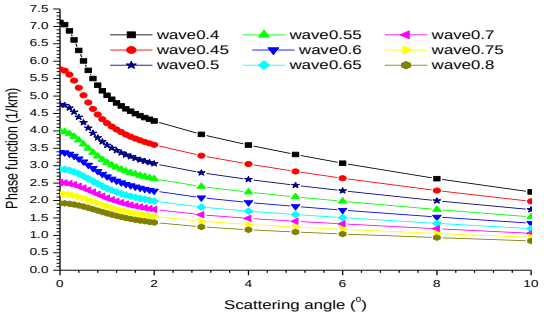

Figure 15(b): A graph of Phase functions against scattering angles at 98% RH WASO Model 2

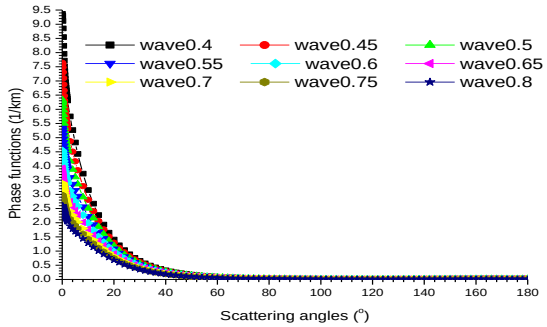

Figure 16(a): A graph of Phase functions against scattering angles at 99% RH WASO Model 2

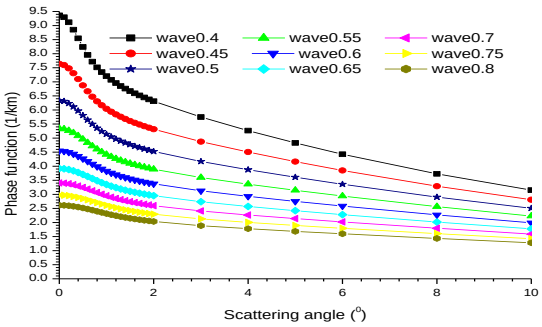

Figure 16(b): A graph of Phase functions against scattering angles at 99% RH WASO Model 2

Figures 9-16 demonstrate that the phase function decreases with increasing scattering angles, adhering to the inverse power law. The phase functions are more pronounced at lower scattering angles, and this is because as the scattering angles increase, the scattering cross-section for forward scattering decreases, resulting in a reduced phase function. When all the plots are compared, it is evident that the phase function increases with increasing relative humidity RH. This is attributed to aerosol swelling due to water uptake, which increases the scattering cross-section and enhances forward scattering. The phase function decreases with increasing wavelength because longer wavelengths are more susceptible to aerosol absorption. This increased absorption reduces the amount of scattered light, leading to a decrease in forward scattering and, consequently, a reduction in the phase function, as can be seen more clearly from figures 9b-16b.

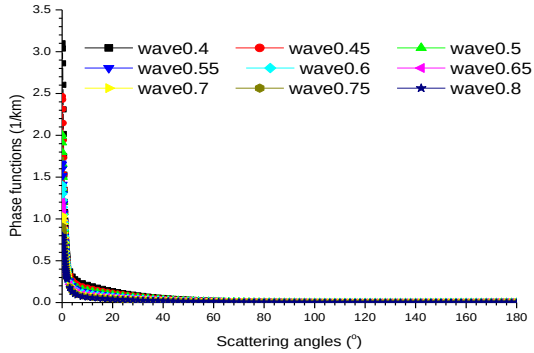

Figure 17(a): A graph of Phase functions against scattering angles at 0% RH WASO Model 3

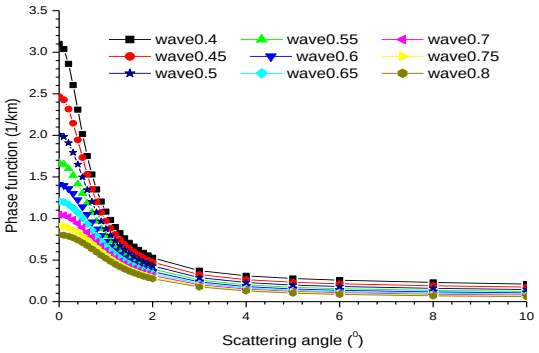

Figure 17(b): A graph of Phase functions against scattering angles at 0% RH WASO Model 3

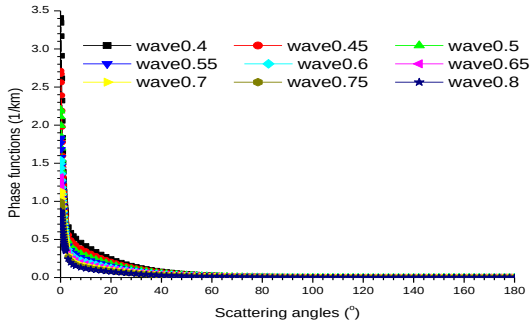

Figure 18(a): A graph of Phase functions against scattering angles at 50% RH WASO Model 3

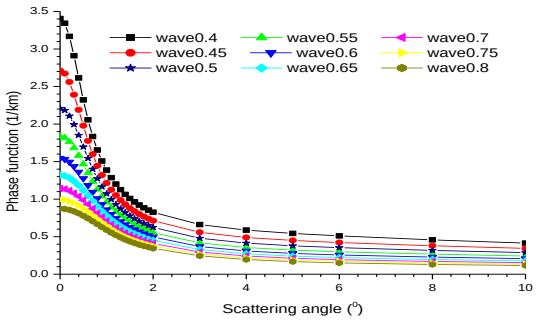

Figure 18(b): A graph of Phase functions against scattering angles at 50% RH WASO Model 3

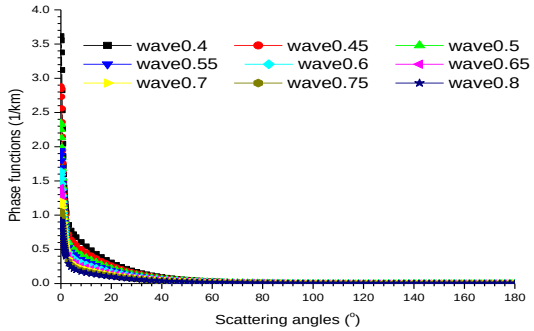

Figure 19(a): A graph of Phase functions against scattering angles at 70% RH WASO Model 3

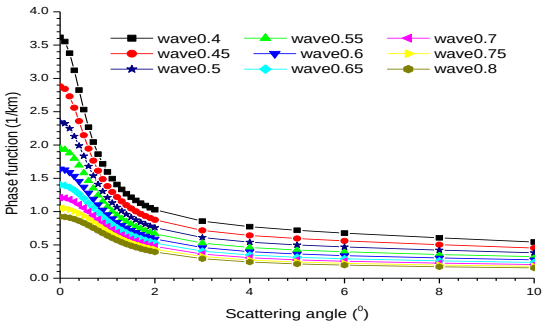

Figure 19(b): A graph of Phase functions against scattering angles at 70% RH WASO Model 3

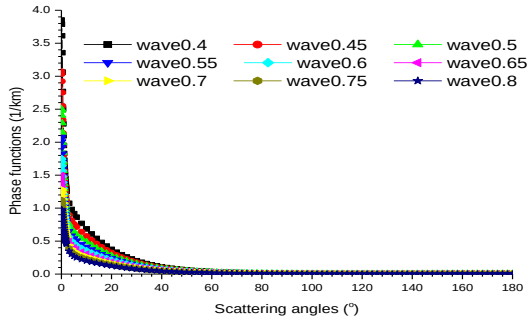

Figure 20(a): A graph of Phase functions against scattering angles at 80% RH WASO Model 3

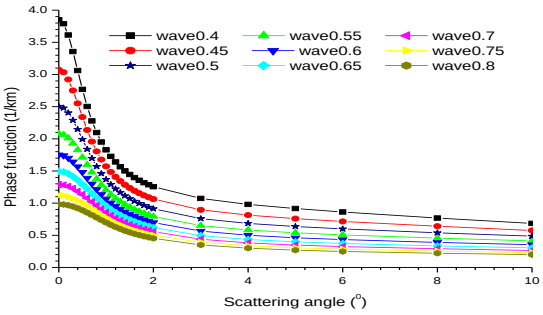

Figure 20(b): A graph of Phase functions against scattering angles at 80% RH WASO Model 3

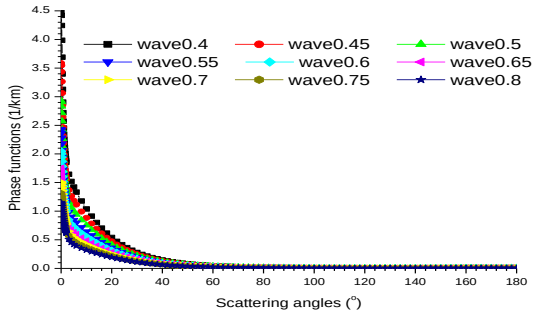

Figure 21(a): A graph of Phase functions against scattering angles at 90% RH WASO Model 3

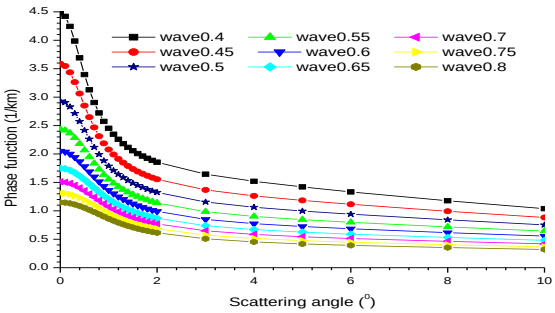

Figure 21(b): A graph of Phase functions against scattering angles at 90% RH WASO Model 3

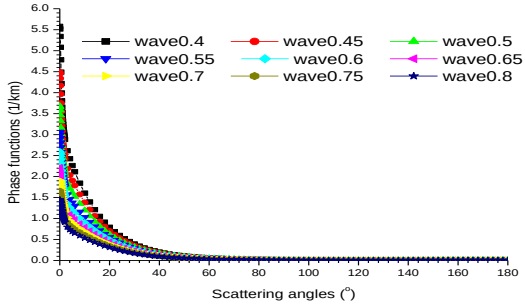

Figure 22(a): A graph of Phase functions against scattering angles at 95% RH WASO Model 3

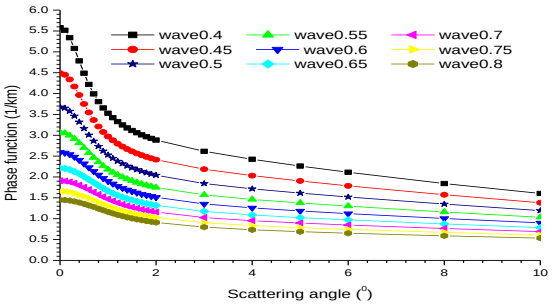

Figure 22(b): A graph of Phase functions against scattering angles at 95% RH WASO Model 3

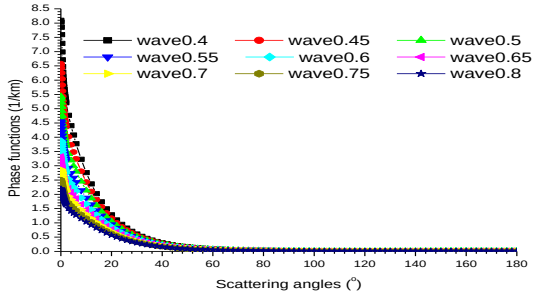

Figure 23(a): A graph of Phase functions against scattering angles at 98% RH WASO Model 3

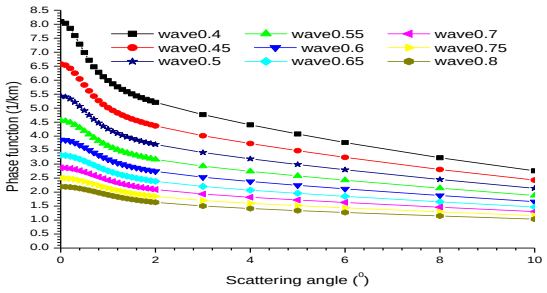

Figure 23(b): A graph of Phase functions against scattering angles at 98% RH WASO Model 3

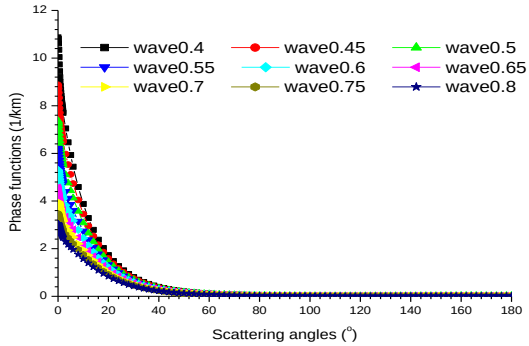

Figure 24(a): A graph of Phase functions against scattering angles at 99% RH WASO Model 3

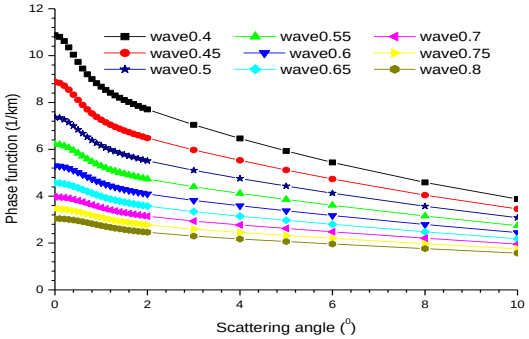

Figure 24(b): A graph of Phase functions against scattering angles at 99% RH WASO Model 3

Figures 17–24 illustrate that the phase functions decrease as the scattering angle increases, following an inverse power law. The phase function is more pronounced at lower scattering angles, and as the scattering angle increases, the forward scattering cross-section decreases, leading to a reduced phase function. Comparison of all the plots reveals that the phase function increases with higher relative humidity (RH). This increase is attributed to aerosol swelling due to water uptake, which enhances the scattering cross-section and forward scattering. The phase function decreases with increasing wavelength because longer wavelengths are more susceptible to aerosol absorption. This increased absorption reduces the amount of scattered light, leading to a decrease in forward scattering and, consequently, a reduction in the phase function, as shown in Figures 17b–24b.

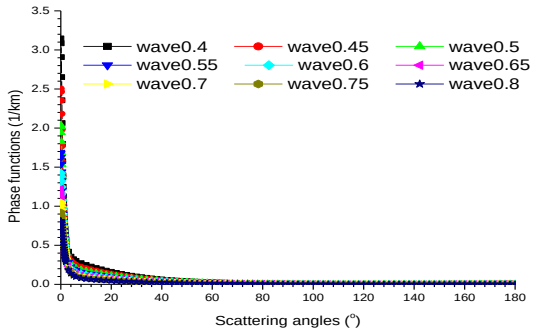

Figure 25(a): A graph of Phase functions against scattering angles at 0% RH WASO Model 4

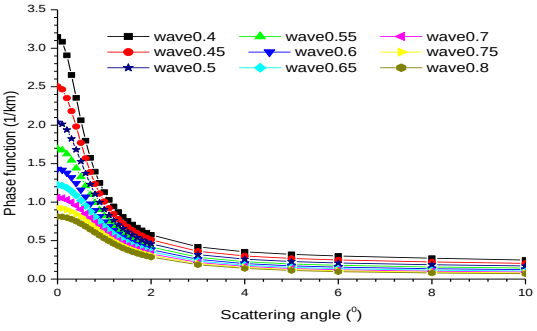

Figure 25(b): A graph of Phase functions against scattering angles at 0% RH WASO Model 4

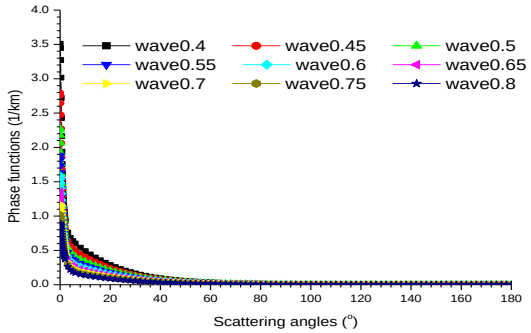

Figure 26(a): A graph of Phase functions against scattering angles at 50% RH WASO Model 4

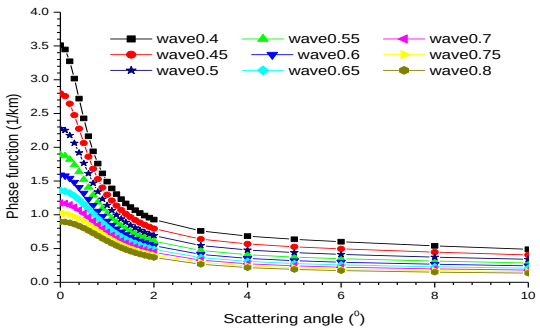

Figure 26(b): A graph of Phase functions against scattering angles at 50% RH WASO Model 4

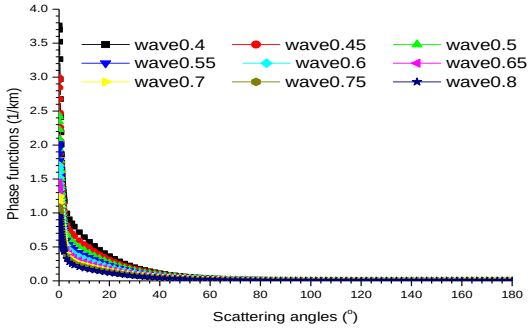

Figure 27(a): A graph of Phase functions against scattering angles at 70% RH WASO Model 4

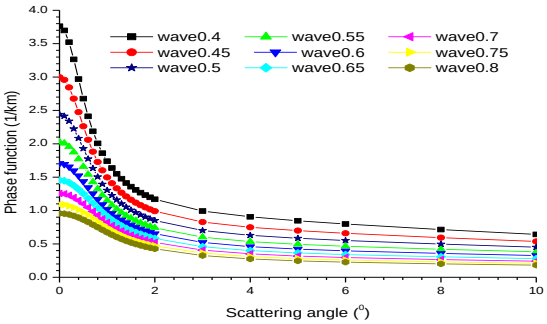

Figure 27(b): A graph of Phase functions against scattering angles at 70% RH WASO Model 4

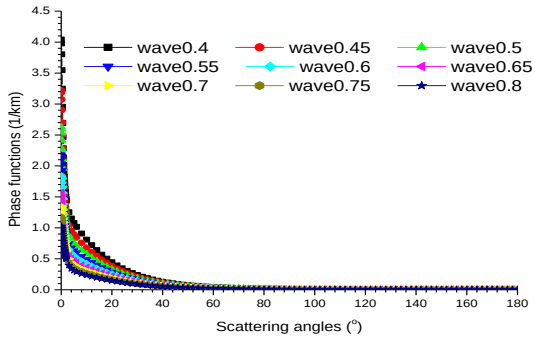

Figure 28(a): A graph of Phase functions against scattering angles at 80% RH WASO Model 4

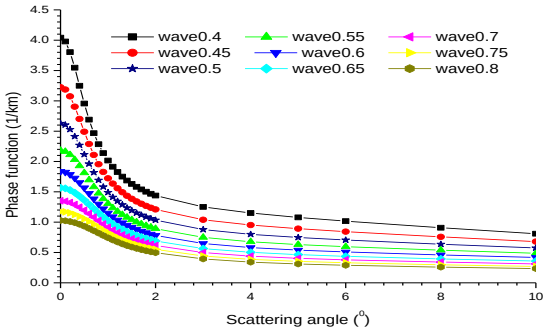

Figure 28(b): A graph of Phase functions against scattering angles at 80% RH WASO Model 4

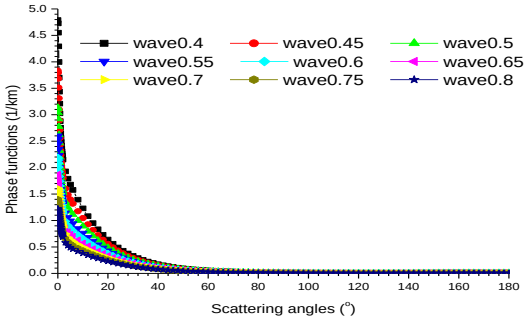

Figure 29(a): A graph of Phase functions against scattering angles at 90% RH WASO Model 4

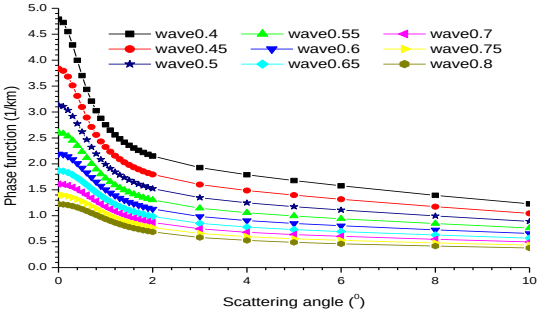

Figure 29(b): A graph of Phase functions against scattering angles at 90% RH WASO Model 4

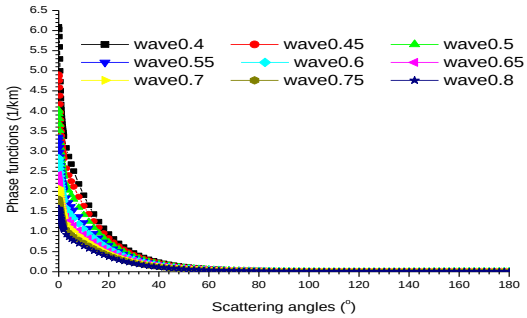

Figure 30(a): A graph of Phase functions against scattering angles at 95% RH WASO Model 4

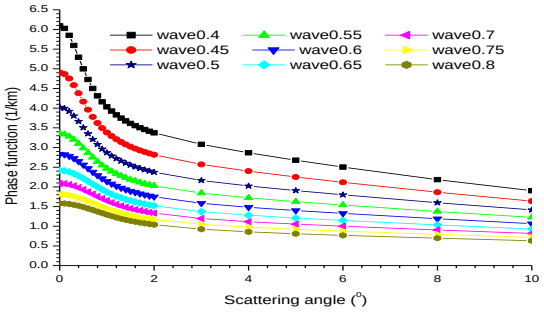

Figure 30(b): A graph of Phase functions against scattering angles at 95% RH WASO Model 4

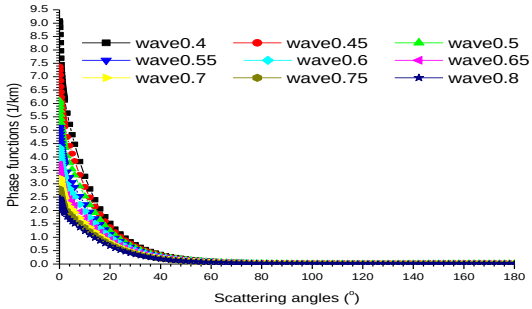

Figure 31(a): A graph of Phase functions against scattering angles at 98% RH WASO Model 4

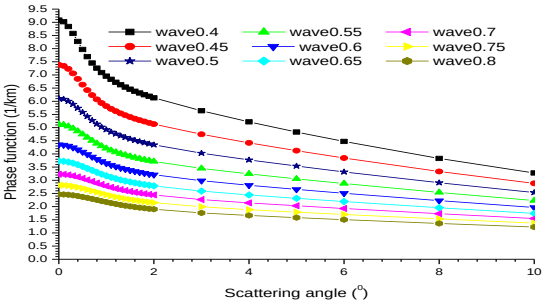

Figure 31(b): A graph of Phase functions against scattering angles at 98% RH WASO Model 4

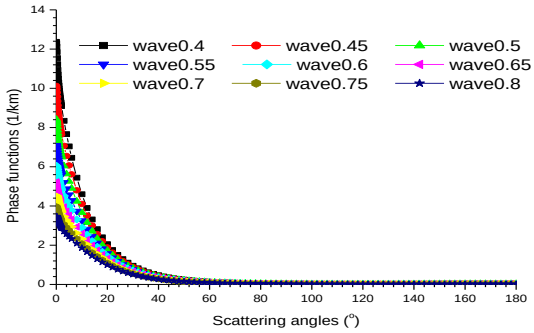

Figure 32(a): A graph of Phase functions against scattering angles at 99% RH WASO Model 4

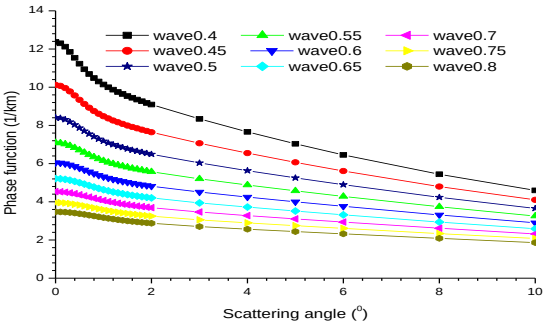

Figure 32(b): A graph of Phase functions against scattering angles at 99% RH WASO Model 4

These figures reveal that the phase function diminishes as the scattering angle increases, consistent with an inverse power law. At lower scattering angles, the phase function is more pronounced; however, as the scattering angle increases, the forward scattering cross-section decreases, leading to a reduction in the phase function. Upon comparing all the plots, it is evident that the phase functions increase with increase in relative humidity (RH). This enhancement is attributed to aerosol swelling due to water uptake, which increases the scattering cross-section and forward scattering. The phase functions decrease with increasing wavelength because longer wavelengths are more susceptible to aerosol absorption. This increased absorption reduces the amount of scattered light, leading to a decrease in forward scattering and, consequently, a reduction in the phase function, as shown in Figures 25b–32b.

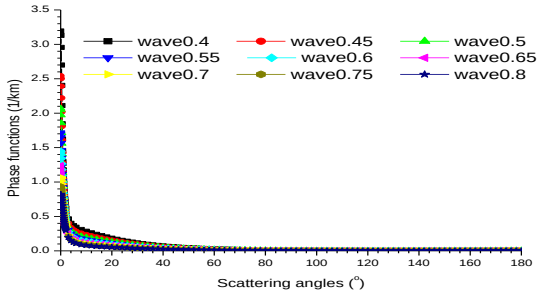

Figure 33(a): A graph of Phase functions against scattering angles at 0% RH WASO Model 5

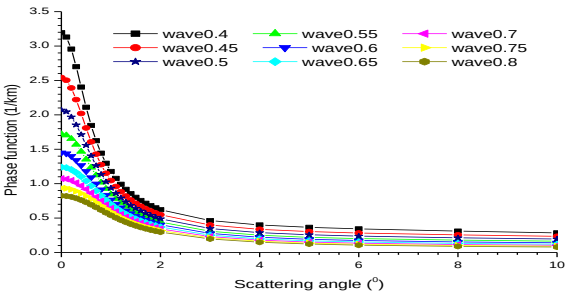

Figure 33(b): A graph of Phase functions against scattering angles at 0% RH WASO Model 5

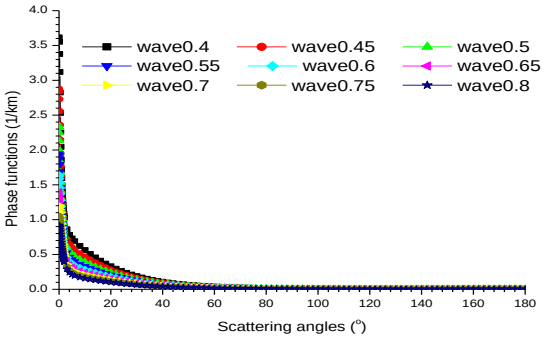

Figure 34(a): A graph of Phase functions against scattering angles at 50% RH WASO Model 5

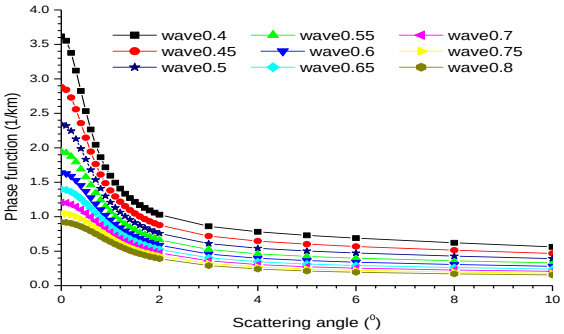

Figure 34(b): A graph of Phase functions against scattering angles at 50% RH WASO Model 5

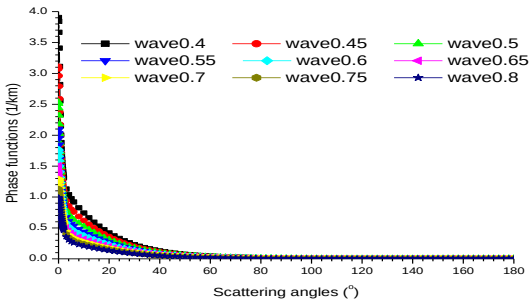

Figure 35(a): A graph of Phase functions against scattering angles at 70% RH WASO Model 5

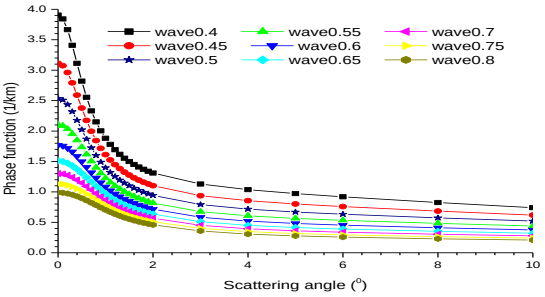

Figure 35(b): A graph of Phase functions against scattering angles at 70% RH WASO Model 5

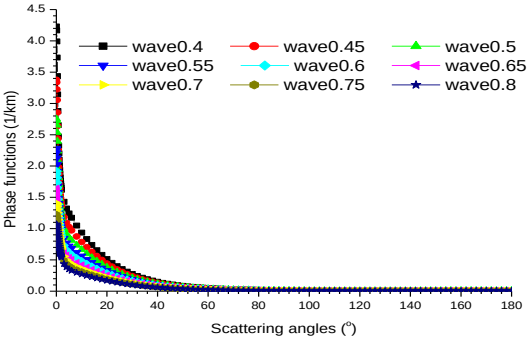

Figure 36(a): A graph of Phase functions against scattering angles at 80% RH WASO Model 5

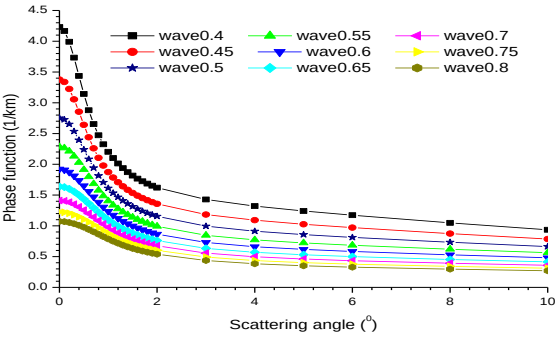

Figure 36(b): A graph of Phase functions against scattering angles at 80% RH WASO Model 5

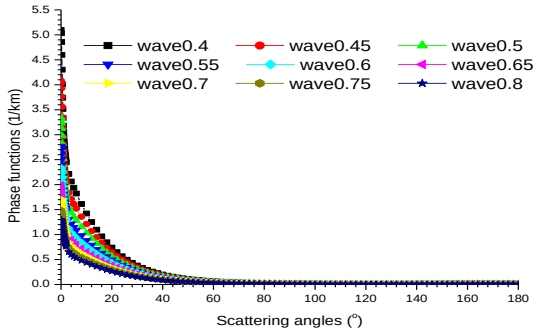

Figure 37(a): A graph of Phase functions against scattering angles at 90% RH WASO Model 5

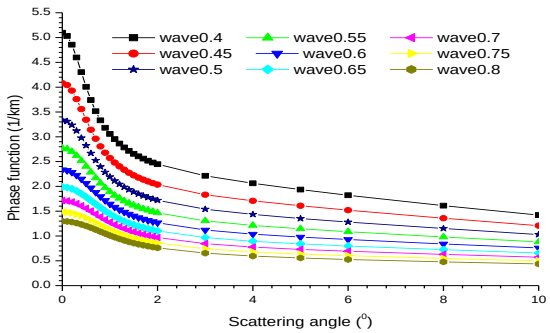

Figure 37(b): A graph of Phase functions against scattering angles at 90% RH WASO Model 5

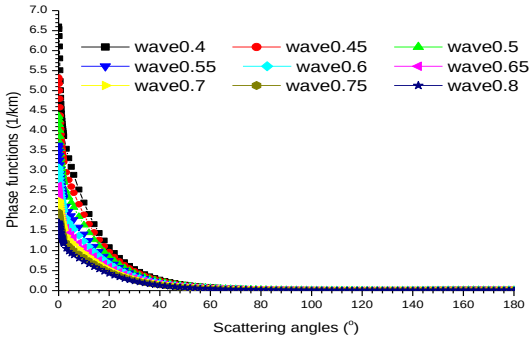

Figure 38(a): A graph of Phase functions against scattering angles at 95% RH WASO Model 5

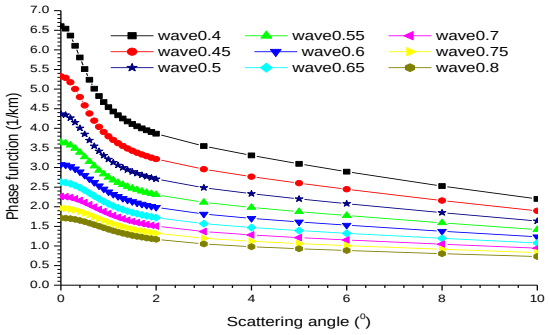

Figure 38(b): A graph of Phase functions against scattering angles at 95% RH WASO Model 5

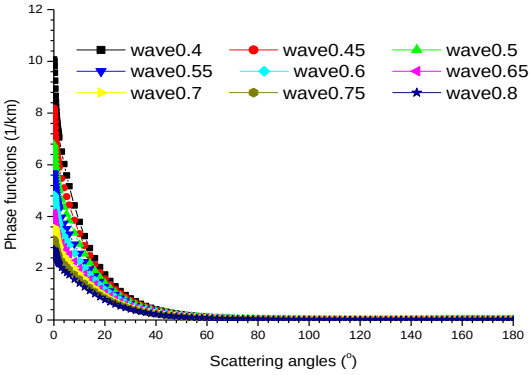

Figure 39(a): A graph of Phase functions against scattering angles at 98% RH WASO Model 5

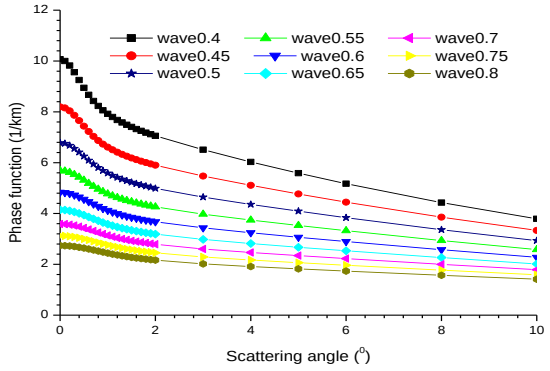

Figure 39(b): A graph of Phase functions against scattering angles at 98% RH WASO Model 5

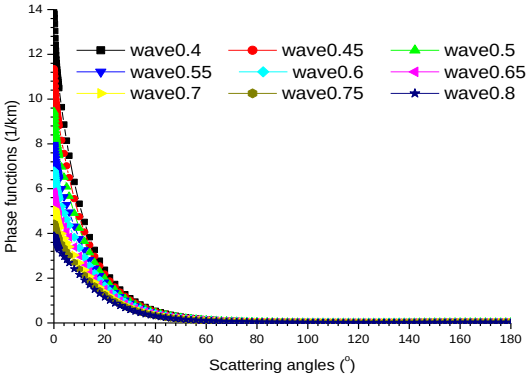

Figure 40(a): A graph of Phase functions against scattering angles at 99% RH WASO Model 5

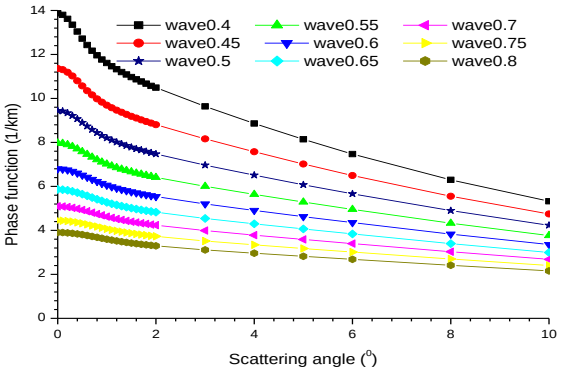

Figure 40(b): A graph of Phase functions against scattering angles at 99% RH WASO Model 5

These plots show that the phase function declines with increasing scattering angle, following an inverse power law. It is more prominent at smaller scattering angles, but as the angle grows, the forward scattering cross-section decreases, which in turn lowers the phase function. A comparison across all the figures indicates that the phase function increases with increasing relative humidity (RH). This trend is due to aerosol particles absorbing moisture and swelling, which enhances both the scattering cross-section and forward scattering. The phase function diminishes at longer wavelengths, as these are more prone to aerosol absorption. This absorption reduces the intensity of scattered light, thereby weakening forward scattering and lowering the phase function, particularly evident in Figures 33b-40b.

The phase functions increase with increasing concentrations of water-soluble aerosols. This is because higher concentrations of water-soluble aerosols enhance aerosol-aerosol interactions, leading to the formation of larger and more complex particles. These particles have a greater scattering cross-section, resulting in increased scattering efficiency and a higher phase function.

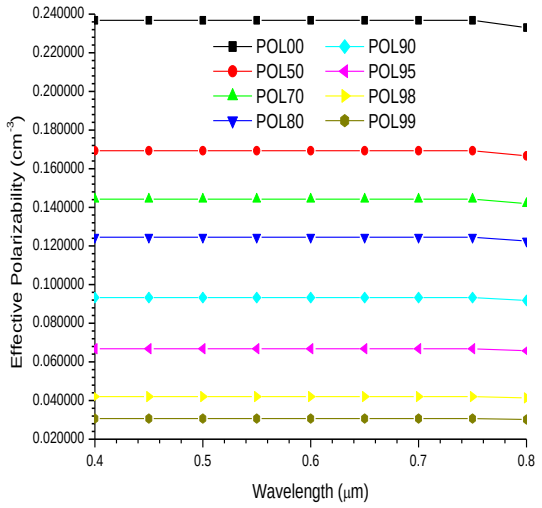

Figure 41: A graph of Effective Polarizability against Wavelength for WASO Model 1

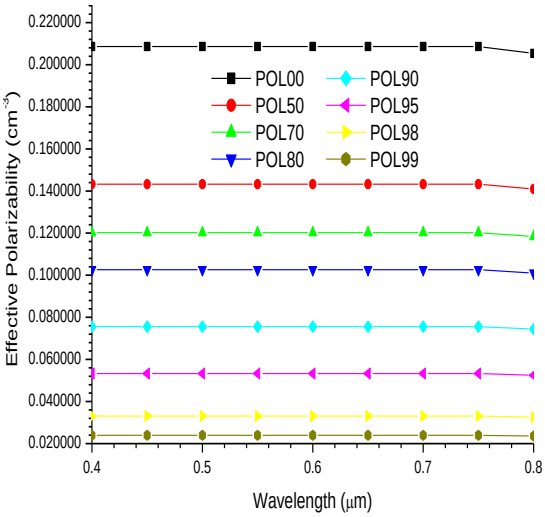

Figure 42: A graph of Effective Polarizability against Wavelength for WASO Model 2

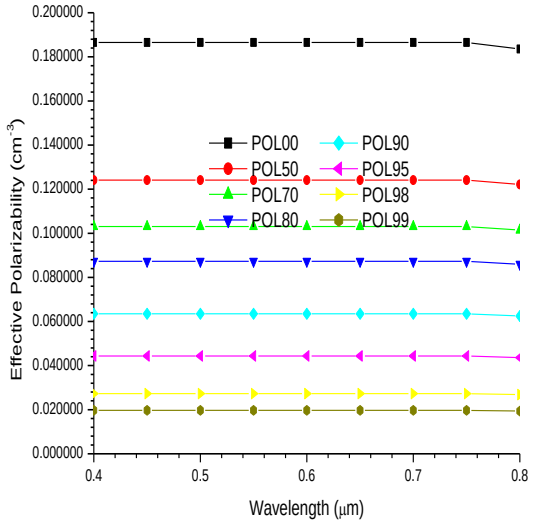

Figure 43: A graph of Effective Polarizability against Wavelength for WASO Model 3

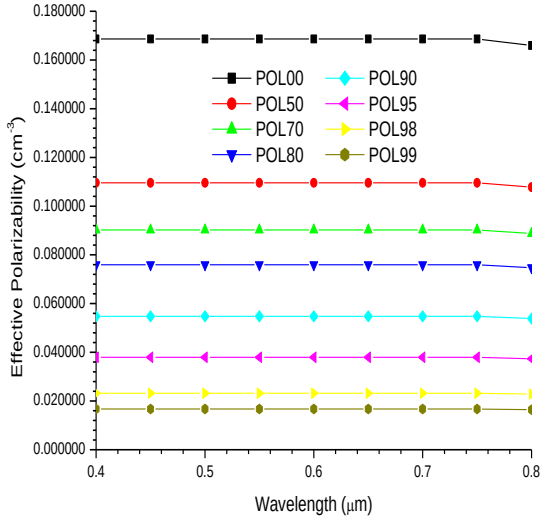

Figure 44: A graph of Effective Polarizability against Wavelength for WASO Model 4

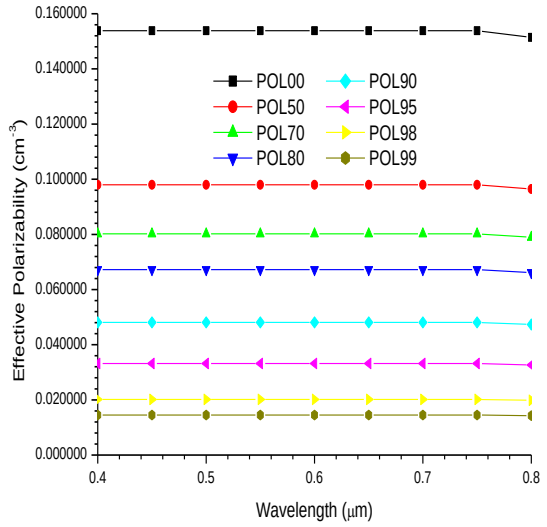

Figure 45: A graph of effective Polarizability against Wavelength for WASO Model 5

Figures 41 to 45 show that the effective polarizability remains constant despite increasing wavelength. This may seem counterintuitive, as the increase in wavelength leads to a decrease in the aerosol size parameter, which would normally decrease polarizability. However, the increased water uptake and aerosol-aerosol interactions at longer wavelengths compensate for this effect, maintaining a constant effective polarizability. The effective polarizability decreases with increasing relative humidity (RH) due to water-soluble aerosols absorbing water vapour, resulting in increased particle size. However, this decrease in effective polarizability is attributed to aerosol swelling as RH increases. The effective polarizability of aerosols decreases with increasing concentrations of water-soluble aerosols. This decrease is attributed to the higher concentration of water-soluble aerosols, which leads to increased scattering and water uptake. As a result, a shielding effect is created, which reduces the effective polarizability by limiting the interaction between the aerosol particles and the incident light.

4. Conclusion

This work investigated the effects of relative humidity, wavelength, and water-soluble aerosol concentrations on the phase functions and effective polarizabilities of urban aerosols. The results showed that phase functions and effective polarizabilities are highly sensitive to scattering angles, relative humidity, wavelength, and aerosol concentration. The phase function decreases with increasing scattering angles due to reduced forward scattering, consistent with the findings of Mishchenko *et al.* (2002). The phase functions decrease with increasing wavelength, due to increased aerosol absorption, which reduces scattered light and forward scattering, as suggested by Pollack and Cuzzi, (1980). The phase function increases with increasing relative humidity, attributed to aerosol swelling and enhanced forward scattering, as observed by Ferrare *et al*., (1998). Furthermore, the phase function increases with increasing concentrations of water-soluble aerosols, due to enhanced aerosol-aerosol interactions and the formation of larger, more complex particles with greater scattering cross-sections, as reported by Liu *et al*., (2012).

The effective polarizability of aerosols decreases with increasing concentrations of water-soluble aerosols. This decrease is attributed to the higher concentration of aerosols, which leads to increased scattering and water uptake, resulting in a shielding effect that reduces the effective polarizability. This shielding effect limits the interaction between aerosol particles and incident light, consistent with the findings of Petters *et al*. (2007). Furthermore, effective polarizabilities decrease with increasing relative humidity (RH) due to water-soluble aerosols absorbing water vapor, resulting in increased particle size. This decrease in effective polarizability is attributed to aerosol swelling as RH increases, as observed by Moosmüller *et al*., (2009). Effective polarizabilities remain relatively constant despite increasing wavelength. Although the increase in wavelength would normally decrease polarizability due to a decrease in the aerosol size parameter, increased water uptake and aerosol-aerosol interactions at longer wavelengths appear to compensate for this effect, maintaining a relatively constant effective polarizability, as suggested by Seinfeld *et al*., (2016).

References

1. Anderson, T. L., R. J. Charlson, S. E. Schwartz, R. Knutti, O. Boucher, H. Rodhe, and J. Heintzenberg (2003). *Climate forcing by aerosols a hazy picture. Science 300*, 1103.
2. Ferrare, R. A., Melfi, S. H., Whiteman, D. N., Evans, K. D., Schmid, B., & Kaufman, Y. J. (1998). A comparison of water vapor measurements made by Raman lidar and radiosondes. *Journal of Geophysical Research: Atmospheres*, *103* (D16), 18705-18716.
3. Hess, M., Koepke, P., & Schult, I. (1998). Optical properties of aerosols and clouds: The software package OPAC. *Bulletin of the American Meteorological Society*, 79(5), 831–844. doi: 10.1175/1520-0477(1998)079<0831:OPOAAC>2.0.CO;2
4. Koepke, P., Gaasteiger, J., and Hess, M. (2015). Optical properties of desert aerosol with non-spherical mineral particles: data incorporate to OPAC. Atmospheric Chemistry and Physics, 15, 5947 – 5956. Doi: 10.5194/acp-15-5947-2015
5. Lindqvist H., Jokinen O., Kandler K., Scheuvens D., and Nousiainen T. (2014): Single Scattering by realistic, inhomogeneous mineral dust particles with stereogrammetric

shapes. *Atmos. Chem. Phys.*, 14.143-157 doi: 10.5194/acp-14-143-2014.

6. Liu, X., Huey, L. G., Yokelson, R. J., Selimovic, V., Simpson, I. J., & Blake, D. R. (2012). Airborne measurements of western U.S. wildfire emissions: Comparison with prescribed burning and urban emissions. Journal of Geophysical Research: Atmospheres, 117(D15), D15303.
7. Mishchenko, M. I., Travis, L. D., & Lacis, A. A. (2002). Scattering, absorption, and emission of light by small particles. Cambridge University Press.
8. Moosmüller, H., Chakrabarty, R. K., & Arnott, W. P. (2009). Aerosol light scattering and absorption: Effects of relative humidity. Journal of Quantitative Spectroscopy and Radiative Transfer, 110(11), 787-796.
9. Petters, M. D., & Kreidenweis, S. M. (2007). A single parameter representation of hygroscopic growth and cloud condensation nucleus activity. Atmospheric Chemistry and Physics, 7(8), 1961-1971.
10. Pollack, J. B., & Cuzzi, J. N. (1980). Scattering by nonspherical particles of size comparable to the wavelength. Journal of the Optical Society of America, 70(10), 1152-1161.
11. Schwartz, S. E. and M. O. Andreae (1996). Uncertainty in climate change caused by aerosols. *Science 272*, 1121-1122.
12. Seinfeld, J. H., & Pandis, S. N. (2016). Atmospheric chemistry and physics: From air pollution to climate change. John Wiley & Sons.
13. Shettle, E. P., and R. W. Fenn, (1979): Models for the aerosols of the lower atmosphere and the effects of humidity variations on their optical properties. *AFGL-TR*-79-0214, 94 pp. [Available from AFCRL, Hanscom Field, Bedford, MA 01731.]
14. Smith, A. B., & Johnson, C. D. (2010). Optical properties of aerosols: A review. *Journal of Atmospheric Sciences*, 67(3), 417–447. doi: 10.1175/2009JAS3087·1